Voltage-Dependent Membrane Capacitance in Rat Pituitary Nerve Terminals Due to Gating Currents

Gordan Kilic* and Manfred Lindau†

*University of Colorado Medical School, Department of Medicine, Denver, Colorado 80262, and †Cornell University, School of Applied and Engineering Physics, Ithaca, New York 14853 USA

ABSTRACT We investigated the voltage dependence of membrane capacitance of pituitary nerve terminals in the whole-terminal patch-clamp configuration using a lock-in amplifier. Under conditions where secretion was abolished and voltage-gated channels were blocked or completely inactivated, changes in membrane potential still produced capacitance changes. In terminals with significant sodium currents, the membrane capacitance showed a bell-shaped dependence on membrane potential with a peak at ~ -40 mV as expected for sodium channel gating currents. The voltage-dependent part of the capacitance showed a strong correlation with the amplitude of voltage-gated Na^+ currents and was markedly reduced by dibucaine, which blocks sodium channel current and gating charge movement. The frequency dependence of the voltage-dependent capacitance was consistent with sodium channel kinetics. This is the first demonstration of sodium channel gating currents in single pituitary nerve terminals. The gating currents lead to a voltage- and frequency-dependent capacitance, which can be well resolved by measurements with a lock-in amplifier. The properties of the gating currents are in excellent agreement with the properties of ionic Na^+ currents of pituitary nerve terminals.

INTRODUCTION

Nerve terminals of magnocellular neurons secrete the hormones vasopressin (AVP) or oxytocin in response to electrical stimulation. During stimulation Ca^{2+} enters through voltage-dependent Ca^{2+} channels leading to fusion of secretory vesicles with the cell membrane and discharge of hormones into the extracellular space. Patch-clamp capacitance measurements (Neher and Marty, 1982) have been used to monitor exocytosis from single nerve terminals (Fidler Lim et al., 1990; Giovannucci and Stuenkel, 1997; Hsu and Jackson, 1996; Lindau et al., 1992). Because the plasma membrane capacitance is directly proportional to the plasma membrane area, the capacitance can be used to measure changes in plasma membrane area due to incorporation (exocytosis) or retrieval (endocytosis) of vesicle membrane (Neher and Marty, 1982). For high-resolution capacitance measurements typically a sine wave (800-Hz, 10–100-mV amplitude) is added to the command voltage and the admittance is analyzed with a two-phase lock-in amplifier (Gillis, 1995; Lindau and Neher, 1988; Neher and Marty, 1982). At the correct phase setting the in-phase and out-of-phase lock-in amplifier output signals change proportional to the changes in membrane conductance and membrane capacitance, respectively (Neher and Marty, 1982).

Time-resolved capacitance measurements provide the unique opportunity to measure the exocytotic response to defined depolarizing stimuli under voltage-clamp conditions. However, the capacitance measurement during depolarization is usually discarded because other voltage-dependent phenomena affect the admittance of the cell or nerve terminal (Neher and Marty, 1982). One such contribution comes from the kinetics of voltage-dependent currents (Cole, 1972). During lock-in measurements the activation of voltage-dependent channels in response to a sinusoidal voltage leads to frequency-dependent and phase-shifted currents. These currents can produce apparent changes in capacitance and lead to misinterpretation of capacitance changes measured with a lock-in amplifier (Debus et al., 1995). Major changes due to voltage-dependent currents occur in capacitance recordings when the kinetic rate constant (k) of voltage-gated channels is similar to the angular frequency (ω) of the sine wave (Cole, 1972; Debus et al., 1995). Depending on the kinetic properties of membrane conductances, the expected amplitude of such phenomena can be estimated (Debus et al., 1995).

In addition to the contribution from voltage-dependent currents to the membrane capacitance, the capacitance of neurons shows voltage- and frequency-dependent contributions from gating currents arising from the charge redistribution in channel proteins that occur during transitions between conformational states (Armstrong and Bezanilla, 1973, 1974; Bezanilla et al., 1991; Fernandez et al., 1982). In chromaffin cells, after brief depolarizing pulses transient capacitance increases were observed, which then slowly returned to the baseline (Horrigan and Bookman, 1994). This phenomenon was reflecting a change in gating currents as Na^+ channels were recovering from inactivation (Horrigan and Bookman, 1994).

To determine the contribution of gating currents to the membrane capacitance in pituitary nerve terminals, we performed lock-in capacitance measurements in the whole-

Received for publication 16 June 2000 and in final form 21 December 2000.

Address reprint requests to Dr. Manfred Lindau, Cornell University, School of Applied and Engineering Physics, 217 Clark Hall, Ithaca, NY 14853. Tel.: 607-255-5264; Fax: 607-255-7658; E-mail: ml95@cornell.edu.

0006-3495/01/03/1220/10 $2.00

terminal configuration under conditions where exocytosis was inhibited and ionic currents were blocked or inactivated. We found that under these conditions the nerve terminal capacitance was voltage dependent in the range between −120 and +40mV. The main contribution to this voltage-dependent capacitance came from Na^+ channel gating currents.

MATERIALS AND METHODS

Preparation of nerve terminals

Nerve terminals were prepared from adult Sprague-Dawley rats as described previously (Cazalis et al., 1987; Lindau et al., 1992). After decapitation, the neurohypophysis was isolated and placed in a physiological saline containing (in mM) 140 NaCl, 5 KCl, 5 $NaHCO_3$, 1 $MgCl_2$, 2.2 $CaCl_2$, 10 D-glucose, 0.01% bovine serum albumin, and 10 HEPES (pH 7.25 adjusted with NaOH) at 37°C. The neural lobe was isolated under a microscope and homogenized in 100 μl of a buffer containing (in mM) 270 sucrose, 0.01 EGTA, and 10 HEPES (pH 7.25 adjusted with *N*-methyl-D-glucamine hydroxide (NMG-OH)). The homogenate containing nerve terminals detached from their axons was transferred into a recording chamber with the bottom made of a glass coverslip. After terminals were allowed to settle on the coverslip for 1 min, the chamber was washed with solution E1 (see below), which was also used as a bath solution for electrophysiological measurements. Under the microscope, nerve terminals appeared as smooth spherical bodies with diameters of 2–15 μm. Terminals with diameter >8 μm were used for patch-clamp experiments within 2 h after the rat was decapitated.

Solutions for electrophysiology

For patch-clamp experiments nerve terminals were initially placed in external solution E1 containing (in mM) 100 NMG-Cl, 5 KCl, 40 NaCl, 1 $MgCl_2$, 2 $CaCl_2$, 15 D-glucose, and 10 HEPES. After obtaining the whole-terminal configuration E1 was exchanged for solution E2 that contained (in mM) 120 tetraethylammonium chloride, 20 4-aminopyridine, 25 NaCl, 1 $MgCl_2$, 0.05 $CaCl_2$, 0.1 $CdCl_2$, 10 D-glucose, and 10 HEPES. In solution E2 4-aminopyridine was included to block the A current, tetraethylammonium chloride to block other K^+ currents, and Cd^{2+} to block voltage-dependent Ca^{2+} currents. Low [Ca^{2+}] was used to minimize the Ca^{2+} currents that were not completely blocked by Cd^{2+} (Almers and McCleskey, 1984).

Internal (pipette) solution contained (in mM) 125 Cs-glutamate, 25 CsCl, 5 NaCl, 7 $MgCl_2$, 2 ATP-Na_2, 0.1 EGTA, 0.03 cAMP, and 10 HEPES. High free [Mg^{2+}] (~5 mM) was used to block slowly activating voltage-dependent outward currents (Kilic et al., 1996).

The osmolality of all solutions was adjusted to 300 mosM, and the pH of all solution was 7.25. Liquid junction potential between pipette and external solutions was ~12 mV. Membrane potentials were corrected for the liquid junction potential.

Lock-in capacitance measurements

The whole-cell patch-clamp technique was used to perform experiments on isolated nerve terminals. After obtaining whole-terminal configuration, compensation of membrane capacitance and access resistance was done using the EPC-9 (HEKA Electronics, Lambrecht/Pfalz, Germany) patch-clamp amplifier. Capacitance and access resistance were 1.5–4 pF and 7–12 MΩ, respectively.

Capacitance changes were measured with a lock-in amplifier PAR 5210 (Princeton Applied Research, Princeton NJ) using the piecewise linear technique (Gillis, 1995; Lindau and Neher, 1988; Neher and Marty, 1982), except for the dibucaine experiments (see below). A continuous sine wave (rms 10 mV, 800 Hz) was added to the command potential, and the current output from the patch-clamp amplifier was fed into the lock-in amplifier. In some experiments frequencies of 400 Hz and 2 kHz were used to investigate frequency dependence. At correct phase setting, one lock-in output (Y_1) is sensitive to changes in membrane conductance whereas the other output (Y_2) is sensitive to changes in membrane capacitance (Gillis, 1995; Lindau, 1991; Lindau and Neher, 1988; Neher and Marty, 1982). A change of 200 fF in the capacitance compensation of EPC-9 was used to adjust the phase and to calibrate capacitance and conductance measurements as previously described (Lindau, 1991; Lindau et al., 1992). The whole-terminal current and command voltage, both filtered at 100 Hz (to remove the sine wave), and the two outputs of lock-in amplifier were sampled by an A/D converter every 25 ms. To measure voltage-dependent capacitance during lock-in recordings, voltage pulses (2–10 s) were given from a holding potential (H_p) of −82mV.

In experiments with dibucaine, capacitance changes were measured with the software lock-in implemented in the program Pulse Control (Herrington and Bookman, 1994). Sine wave frequency and amplitude were 800 Hz and 30 mV, respectively. Capacitance was determined every 50 ms.

Measurements of Na^+ currents

To investigate the relation between the Na^+ current and voltage-dependent capacitance, the Na^+ current was measured before the measurement of voltage-dependent capacitance. One second before the pulse to measure voltage-dependent capacitance was given, the sine wave was switched off for 200 ms. During this period a 5-ms depolarizing pulse was given to $V_m = -22$ mV. The current response evoked by this pulse was filtered at 29.9 kHz and sampled every 17 μs. Four hyperpolarizing pulses ($V_m = -97$ mV, 5 ms) were also given and current responses stored. These currents were later used for subtraction of leak and capacitive currents using standard methods. A membrane potential of −22 mV was chosen because Na^+ currents were maximal at this pulse potential with the external solution E2 used to block other voltage-dependent currents.

All experiments were done at room temperature (22–24°C). Data analysis was performed using the program IgorPro3 (WaveMetrics, Lake Oswego, OR). The correlation between the maximal amplitudes of Na^+ currents and the membrane capacitance changes at given membrane potential was calculated by linear regression using IgorPro 3.

RESULTS

At a holding potential of −82 mV nerve terminals showed stable membrane capacitance and conductance. Fig. 1 shows capacitance and conductance changes and the whole-terminal current evoked by a 10-s depolarization to −52 mV. Because pipette and bath solutions contained blockers of voltage-gated K^+ and Ca^{2+} channels, the only current observed was the voltage-gated Na^+ current (*bottom trace*). Because the Na^+ current was completely inactivated within a few tens of milliseconds, the long-lasting changes in capacitance and conductance trace cannot be attributed to the presence of voltage-dependent ionic currents. The capacitance change also does not reflect exocytotic activity because under the conditions employed here no significant calcium influx is evoked. To quantify the apparent change in membrane capacitance during a voltage pulse we measured the capacitance change (ΔC_{step}) at 100 ms after the

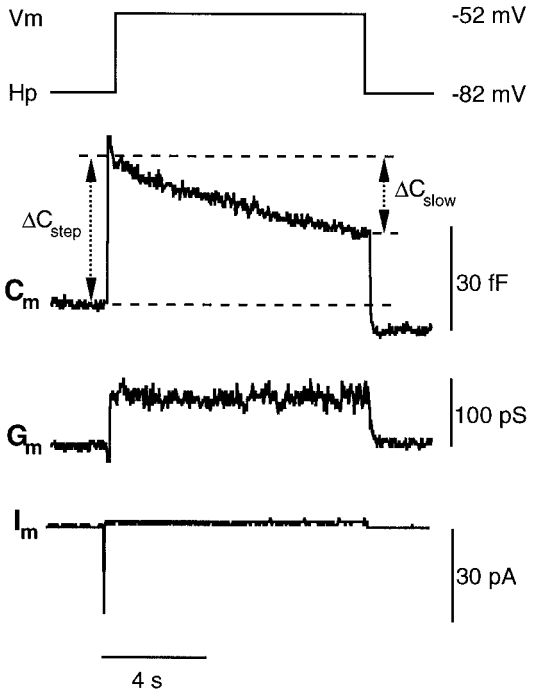

FIGURE 1 Depolarization-induced changes in membrane capacitance, conductance, and current when K^+ and Ca^{2+} channels were blocked. Nerve terminal was depolarized to −52 mV for 10 s (*top trace*). A sine wave voltage (not shown) was superimposed throughout the recording. Whole-terminal current (*bottom trace*) shows an inward spike originating from the activation of voltage-gated Na^+ channels that also produced spikes in capacitance (*top trace*) and conductance (*middle trace*). The spikes were truncated for better visualization of long-lasting capacitance and conductance changes. As Na^+ current inactivates, the changes in capacitance (~40 fF) and conductance (~100 pS) persist throughout the pulse. The early change in capacitance (ΔC_{step}) was measured 100 ms after the beginning of a pulse. The slow decrease in capacitance (ΔC_{slow}) observed during 10-s pulses was also quantified. Holding potential was −82 mV. To remove the sine wave, the whole-terminal current was filtered at 100 Hz.

onset of the voltage pulse. At this time the Na^+ current was fully inactivated and the resulting effects in the C-trace had completely ceased. Following the step-like increase the capacitance trace shows a gradual decline during the pulse. The extent of the decrease during the 10-s pulse (ΔC_{slow}) was also quantified. Upon repolarization the capacitance was slightly below the initial values and then slowly returned to the pre-pulse baseline (not shown). Simultaneously occurring apparent changes in conductance varied between −200 and 200 pS and were not systematically studied here.

Capacitance depends on membrane potential and Na^+ current

To determine the dependence of ΔC_{step} on membrane potential, shorter voltage pulses of 2-s duration were given to various test potentials (Fig. 2). The resulting capacitance

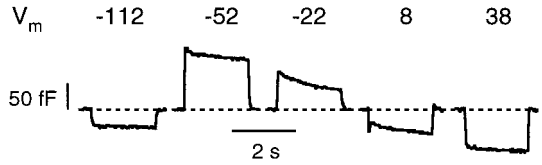

FIGURE 2 Capacitance changes during 2-s pulses to various potentials. Pulses were given to the potentials indicated at the top from a holding potential of −82 mV. Hyperpolarizing ($V_m < -90$ mV) and strong depolarizing ($V_m > 0$ mV) pulses decreased the capacitance. At pulse potentials in the range −70 to 0 mV a capacitance increase is observed. The initial spike in capacitance due to activation of voltage-gated Na^+ currents was truncated in the trace for −52-mV pulse potential. Baseline capacitance of the nerve terminal was 3.3 pF.

changes ΔC_{step} showed a clear voltage dependence being positive for depolarizing potentials from −70 to −20 mV and negative at hyperpolarized or very depolarized (>0 mV) potentials.

To test whether ΔC_{step} in pituitary nerve terminals is related to Na^+ channel gating currents we investigated the correlation of the capacitance changes with the maximum amplitudes of Na^+ currents (I_{Na}) induced by a 5-ms pulse to −22 mV test potential. At this membrane potential I_{Na} was largest with the solutions used here. Among different nerve terminals I_{Na} was highly variable. I_{Na} could be as large as 1 nA or could be undetectable. Furthermore, during whole-terminal recording the Na^+ current showed some run-down (Fig. 3 *A*). I_{Na} was thus measured 1 s before each voltage pulse that was given to probe ΔC_{step}. Fig. 3 *B* shows a plot of ΔC_{step} versus I_{Na} pooled from 14 nerve terminals for two different test potentials. At $V_m = -52$ mV as well as at $V_m = -122$ mV a clear correlation was observed between ΔC_{step} and I_{Na} (*solid lines*) with correlation coefficients of 1.0 and −0.8, respectively. To ensure that the correlation was not mainly due to the nerve terminal with the largest ΔC_{step} and I_{Na}, we also performed linear regression omitting the data from this terminal (*dashed lines*). The slopes of the regression lines were not significantly different and the correlation coefficients were 0.9 at $V_m = -52$ mV and −0.55 at $V_m = -122$ mV, indicating that the correlation is robust, at least at $V_m = -52$ mV where ΔC_{step} is largest.

The correlation coefficients (r) obtained for various test potentials are plotted versus test potential in Fig. 3 *C*. In the range V_m from −70 to −10 mV the correlation was close to 1.0. At hyperpolarized potentials ($V_m < -90$mV) capacitance changes were negative and the correlation coefficients were between −0.6 and −0.8, indicating a strong correlation in this potential range. At more strongly depolarized potentials $V_m > -10$ mV, ΔC_{step} was only weakly correlated with the size of the Na^+ currents. These results suggest that Na^+ channel gating currents contribute strongly to ΔC_{step} but that there are also other contributions.

A correlation of ΔC_{step} and I_{Na} could occur accidentally if both are related to some third factor. An obvious possi-

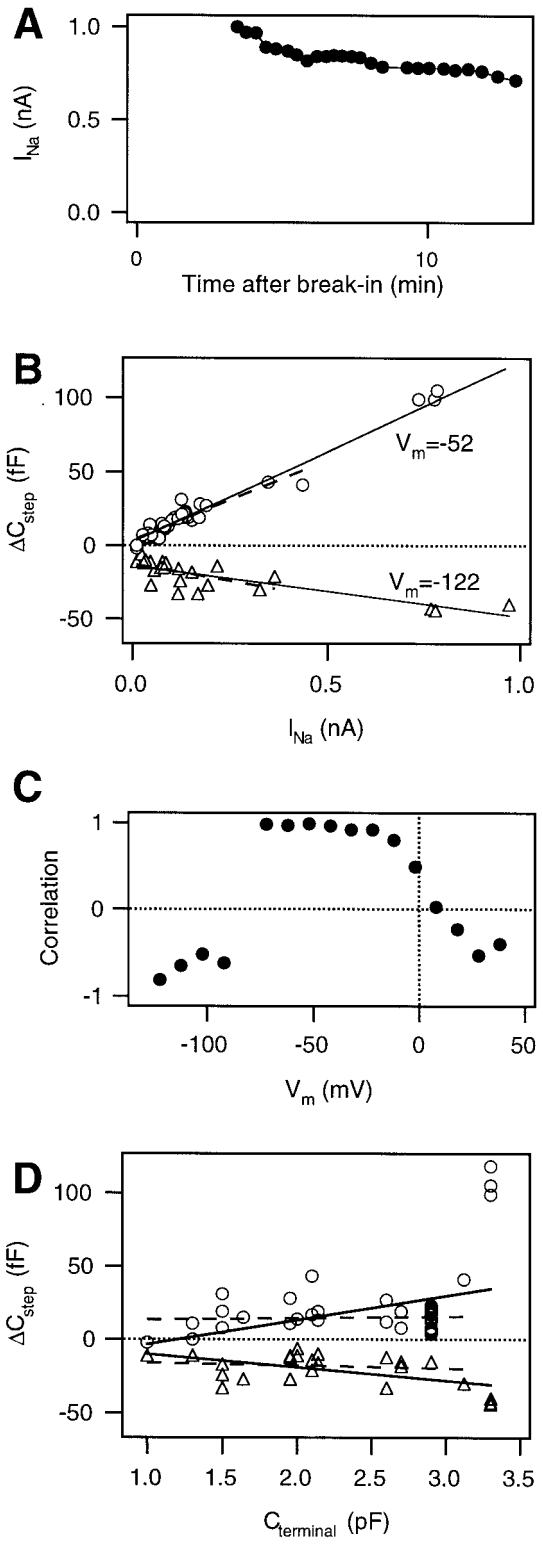

FIGURE 3 Correlation of voltage-dependent capacitance with Na^+ current. (*A*) Na^+ current amplitudes I_{Na} elicited by pulses to −22 mV in the nerve terminal of Fig. 2 decreases with time after obtaining whole-terminal configuration. For the first few minutes of experiments the nerve terminal was not stimulated to allow complete exchange of external solution to E2. (*B*) Capacitance changes ΔC_{step} induced by pulses to −52 mV (○) and to −122 mV (△) compiled from 14 nerve terminals plotted versus I_{Na}. Straight lines were fitted using all data points (*solid lines*) and omitting the data from the terminal with the largest ΔC_{step} (*dashed lines*). Note a strong positive correlation at V_m = −52 mV and a negative correlation at V_m = −122 mV. (*C*) Correlation coefficients obtained from the graphs as in *B* plotted versus membrane potential. Note a strong positive correlation in the potential range from −70 to −10 mV. (*D*) Capacitance changes ΔC_{step} induced by pulses to −52 mV (○) and to −122 mV (△) as in *B* plotted versus total terminal capacitance. Straight lines were fitted to the two data sets using all data points (*solid lines*) and omitting the data from the largest terminal (*dashed lines*).

bility would be total terminal membrane area. We thus analyzed a possible correlation of ΔC_{step} with the total membrane capacitance of the nerve terminal (Fig. 3 *D*). The difference is most obvious for the data points measured at V_m = −52 mV. Linear regression (*solid line*) yields a correlation coefficient of 0.37. The weak correlation exclusively depends on the data from the terminal with the largest ΔC_{step}, which was measured in the terminal with the largest capacitance. If the data from this terminal is omitted in the analysis, then the regression line yields a slope of 0 and a correlation coefficient of 0.06 is obtained. For the data set measured at −122 mV the correlation coefficients were −0.53 and −0.13 when the largest terminal was included or omitted, respectively. ΔC_{step} thus shows a much stronger correlation with I_{Na} than with nerve terminal capacitance.

Further support that ΔC_{step} is due to Na^+ channel gating currents was obtained using the Na^+ channel blocker dibucaine, which also blocks Na^+ channel gating currents (Gilly and Armstrong, 1980; Horrigan and Bookman, 1994). In the presence of 200 μM dibucaine ΔC_{step} was completely abolished. Fig. 4 shows one of three experiments that gave similar results. To quantify the dibucaine effect two pulses from −82 to −52 mV were first given in standard saline E2 followed by two pulses in the presence of 200 μM dibucaine. Both pulses of a pair gave a similar response. The average response in standard saline was ΔC_{step} = 32 ± 11 fF (SD; n = 3). In the presence of dibucaine ΔC_{step} was very small and had a reversed sign (−6 ± 2 fF, SD; n = 3).

To separate the voltage-dependent capacitance due to Na^+ channel gating currents from other voltage-dependent capacitance, we compared capacitance changes in a nerve terminal having particularly large Na^+ currents with those measured in a nerve terminal that did not have any detectable Na^+ current (Fig. 5 *A*). The amplitude of the smallest detectable current at 29.9 kHz bandwidth was ~10 pA. The voltage dependence of ΔC_{step} in these two terminals is shown in Fig. 5 *B*. For the nerve terminal having no detectable Na^+ current (*open circles*) ΔC_{step} was very small at all potentials from −120 to −70mV. At more depolarized potentials a negative ΔC_{step} appeared, reaching −50 to −60 fF for test potentials >0 mV. The value of −8 fF at −52 mV agrees well with that obtained in the presence of dibucaine at the same potential. The voltage dependence of the capacitance changes in this terminal that were not due to

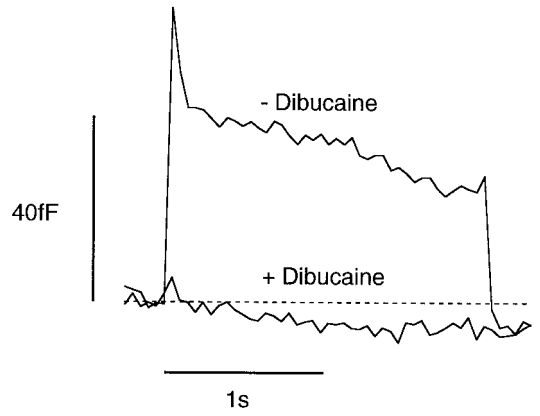

FIGURE 4 Effect of dibucaine on voltage-dependent capacitance. The changes in capacitance were evoked by +30-mV depolarizations (2 s) from holding potential of −82 mV. In the absence of dibucaine (*upper trace*) the ΔC_{step} is positive, similar to Fig. 2. ΔC_{step} measured with the same protocol after addition of dibucaine (200 μM) was very small (*lower trace*).

Na^+ channel gating currents (ΔC_0) could be well fitted (*dashed line*) using a Boltzmann-type equation:

$$\Delta C_0 = \frac{C'}{1 + \exp\left(\frac{V' - V_m}{S}\right)}, \quad (1)$$

where C' is the maximum capacitance change at depolarized potentials, S is the slope factor and V' is the potential

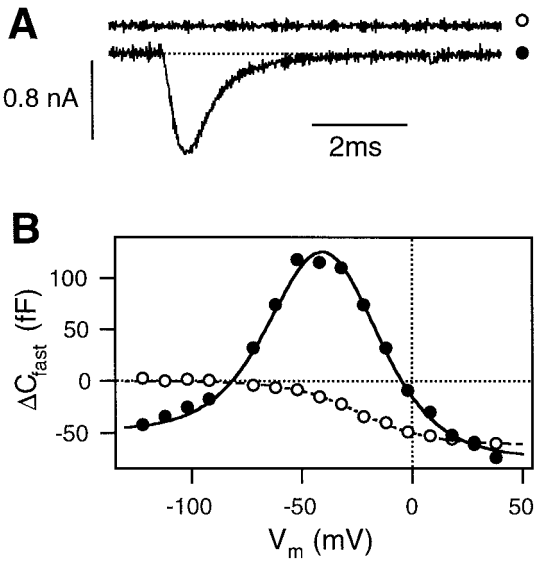

FIGURE 5 Voltage-dependent capacitance in the absence and presence of Na^+ current. (*A*) Whole-terminal currents elicited by 5-ms pulses to −22 mV induced no detectable current in one terminal (*upper trace*) and a strong inward current in the other (*lower trace*). (*B*) Capacitance changes ΔC_{step} for the nerve terminal having no Na^+ current (○) are well fitted with Eq. 1 (*dashed line*). For the nerve terminal with large Na^+ current the ΔC_{step} (●) were well fitted with Eq. 4 (*solid line*).

where the capacitance change is half-maximal. The fit results were $C' = -61$ fF, $V' = -24$ mV, and $S = 16$ mV.

The contribution of gating charges to the membrane capacitance is generally voltage and frequency dependent, and reflects the voltage-dependent kinetics of gating charge movements. For a simple two-state model the capacitance C_G (imaginary part of admittance divided by $\omega = 2\pi f$) due to gating charge movement has the following form (Fernandez et al., 1983; Taylor and Bezanilla, 1979):

$$C_G = \frac{Q_G}{4S_G \cos h^2\left(\frac{V_G - V_m}{2S_G}\right)}, \quad (2)$$

where Q_G is the total gating charge available to move, $S_G = kT/e\alpha$ a slope factor, k the Boltzmann constant, T the absolute temperature, e the elementary charge, and α an experimental parameter equal to the product of the valence of the gating charge and the fraction of the field through which it moves. V_G is the potential at which half of the gating charge is in each state and where the contribution to the capacitance is maximal (Taylor and Bezanilla, 1979). The capacitance change ΔC_G due to a change in gating charge movement associated with a voltage step from the holding potential of −82 mV to membrane potential V_m can then be expressed as

$$\Delta C_G = C_G(V_m) - C_G(V_h) = \frac{Q_G}{4S_G}\left(\frac{1}{\cos h^2\left(\frac{V_G - V_m}{2S_G}\right)} - \frac{1}{\cos h^2\left(\frac{V_G + 82\text{ mV}}{2S_G}\right)}\right), \quad (3)$$

giving the total capacitance change

$$\Delta C_{step} = \Delta C_0 + \frac{Q_G}{4S_G}\left(\frac{1}{\cos h^2\left(\frac{V_G - V_m}{2S_G}\right)} - \frac{1}{\cos h^2\left(\frac{V_G + 82\text{ mV}}{2S_G}\right)}\right). \quad (4)$$

Eq. 4 gives a bell-shaped curve that fit the data points of the terminal with large Na^+ current (Fig. 5 *B*, *filled circles*) extremely well (Fig. 5 *B*, *solid line*). The values V' and S were fixed at −24 mV and 16 mV, respectively. Results for free fit parameters were $C' = -26$ fF, $Q_G = 12$ fC, $V_G = -40$ mV, and $S_G = 16$ mV.

Eq. 4 was used to fit voltage-dependent capacitance changes in all individual nerve terminals. Fig. 6 *A* shows the relation between I_{Na} and gating charge Q_G. Because I_{Na} decreased during the recording from an individual terminal (see Fig. 3 *A*) the mean I_{Na} for each nerve terminal was used in the graph. The gating charge Q_G obtained as the fit parameter is clearly correlated with the size of the Na^+ current, indicating that nerve terminals with larger Na^+

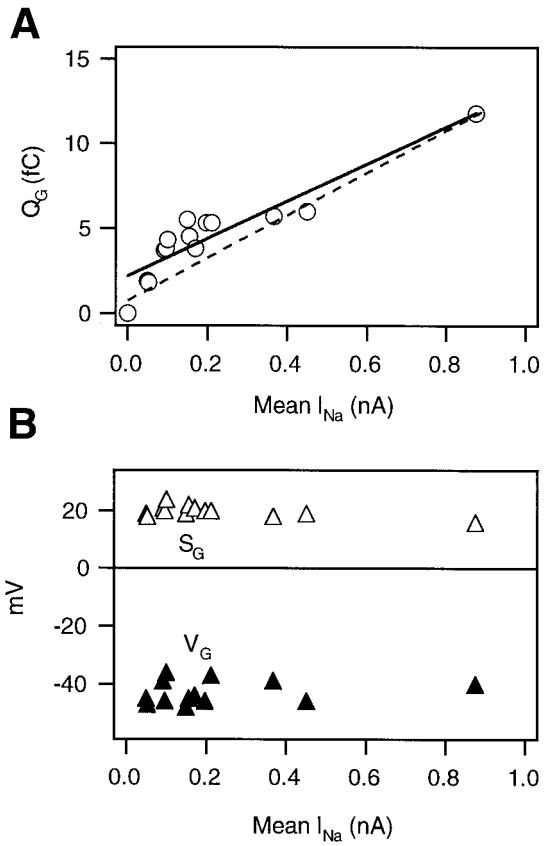

FIGURE 6 Correlation of fit parameters with I_{Na}. (*A*) Gating charge Q_G obtained from fitting Eq. 4 increases with mean Na^+. Linear regression (*solid line*) gives a slope of 11.0 ± 1.3 fC/nA and an intercept of 2.2 ± 0.4 fC. A fit using only the data points from terminals with $I_{Na} > 0.3$ nA (*dashed line*) gives a slope of 12.5 ± 1.4 fC/nA and an intercept of 0.76 ± 0.83 fC. (*B*) Slope factor S_G (△) and the potential of the maximum change V_G (▲) are independent of I_{Na}.

currents contribute more to ΔC_{step}. The data points are well fitted by a straight line with a slope of 11.0 ± 1.3 fC/nA. When only the data points with $I_{Na} > 300$ pA were used, the linear regression was consistent with a line through the origin and a slope of 12.5 ± 1.4 fC/nA. Presumably, the data points for terminals with small I_{Na} are more sensitive to deviations of the additional effects that are assumed to have variable amplitude but always the same shape as in the terminal with no detectable I_{Na}.

As expected, the parameters V_G and S_G show no significant dependence on the size of the Na^+ current and are remarkably constant (Fig. 6 *B*). These parameters are determined by the behavior of the gating charge in the electric field and should not depend on the number of Na^+ channels present in the membrane. Their mean values are $V_G = -42.9 \pm 1.2$ mV and $S_G = 19.8 \pm 0.6$ mV (SEM; $n = 13$), respectively.

The parameter C' that described the size of the contribution to ΔC_{step} not due to Na^+ channel gating charges according to Eq. 1 was included as a free parameter in the fit of Eq. 4. Its value was scattered between −7 and −45 fF and was correlated neither with the size of Na^+ current nor with the total terminal capacitance.

To obtain information on the kinetics of the charge movements underlying the voltage-dependent capacitance, we performed some experiments using different sine wave frequencies in the same terminal. In these experiments, hyperpolarizing pulses to −122 mV were given to minimize contributions from phenomena other than Na^+ channel gating charges (see Fig. 5 *B*). As expected, the voltage-dependent capacitance is also frequency dependent (Fig. 7). Fitting the frequency (f) dependence with a single Debye dispersion (Fernandez et al., 1983; Taylor and Bezanilla, 1979),

$$\frac{\Delta C_{step}}{I_{Na}} = \frac{\Delta C_{step0}}{I_{Na}}\left(\frac{1}{1 + (2\pi f\tau)^2}\right),$$

gave a time constant $\tau = 190 \pm 90$ μs, consistent with Na^+ channel kinetics in pituitary nerve terminals (Jackson and Zhang, 1995).

The slow capacitance decay

The slow capacitance changes following ΔC_{step} measured during 10-s pulses were always negative (see Fig. 1). In Fig. 8 *A* the averaged ΔC_{slow} values from 10 nerve terminals are plotted versus membrane potential. The ΔC_{slow} was largest at potentials around −40 mV. Although this is close to V_G determined as described above for ΔC_{slow} the correlation between ΔC_{slow} at this potential and Na^+ current amplitude was weak, with $r = -0.4$ (Fig. 8 *B*). Interestingly, the correlation coefficient was close to 1 at test potentials around 0 mV. This suggests that ΔC_{slow} is partly related to Na^+ channel gating charges, but that other contributions are

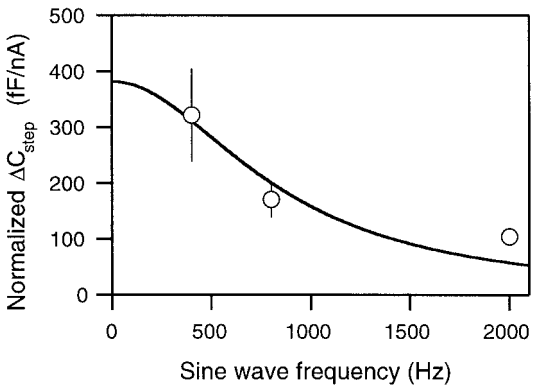

FIGURE 7 Frequency dependence of voltage-dependent capacitance. ΔC_{step} was measured for a voltage step from −82 to −122 mV. To include date from terminals with different I_{Na}, the capacitance changes were normalized to I_{Na} amplitude measured just before the capacitance measurement. The fit assuming a single Debye relaxation (*solid line*) gave a zero frequency value of 380 ± 120 fF/nA and a time constant of 190 ± 90 μs.

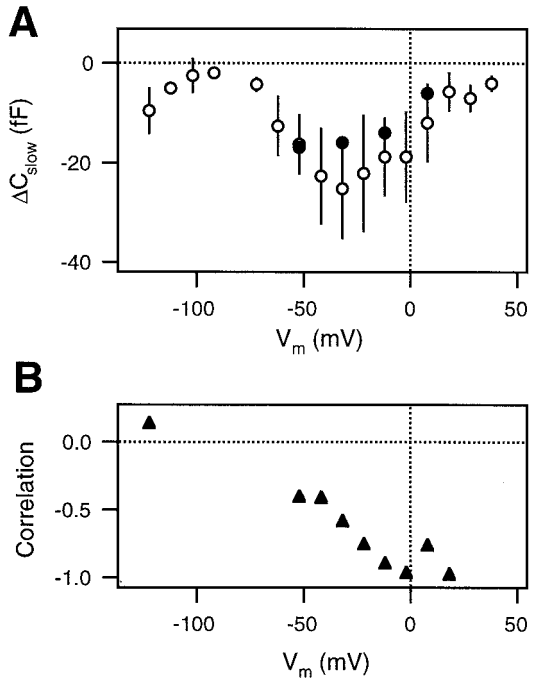

FIGURE 8 Voltage dependence of slow capacitance decrease. (*A*) Averaged ΔC_{slow} values from 10 nerve terminals (○) and from the terminal with no detectable Na^+ current (●) are plotted versus membrane potential. Error bars of mean values are SD. (*B*) Correlation coefficients obtained from linear regression of ΔC_{slow} versus I_{Na} as in Fig. 3 *B* obtained for different pulse potentials.

present as well. In the presence of dibucaine (Fig. 4) and in the nerve terminal of Fig. 5 that showed no Na^+ current, a slow capacitance change was also present (Fig. 8, *open circles*), confirming contributions distinct from Na^+ channel gating charges.

DISCUSSION

There are two main findings in the present study. First, the membrane capacitance of pituitary nerve terminals is voltage dependent. Second, a significant contribution to the voltage-dependent capacitance is due to movement of gating charges of voltage-activated Na^+ channels.

Changes in membrane potential changed nerve terminal capacitance (see Figs. 1 and 2). During sine wave stimulation (used in lock-in recordings) the currents from open voltage-gated channels can produce apparent capacitance changes (Cole, 1972; Debus et al., 1995). With the bath and pipette solutions used here, the only voltage-activated current was a Na^+ current (Fig. 1, *bottom trace*) that completely inactivated within 100 ms (time at which we measured ΔC_{step}). Capacitance changes were also observed at hyperpolarizing potentials at which no voltage-dependent channels were activated (Figs. 2 and 5 *A*), indicating that voltage-dependent capacitance could not originate from currents through voltage-dependent channels.

The composition of solutions was chosen to minimize Ca^{2+} influx through L-type Ca^{2+} channels such that exocytosis is not stimulated. If the capacitance changes were the consequence of exocytosis, then we would expect that they persist for some time after repolarization (Fidler Lim et al., 1990; Giovannucci and Stuenkel, 1997; Hsu and Jackson, 1996; Lindau et al., 1992). However, the capacitance changes observed during 2-s depolarizations were reversed instantaneously upon return to the holding potential (Fig. 2). These results strongly suggest that the voltage-dependent capacitance changes under these experimental conditions are not due to stimulation of exo- or endocytosis resulting in changes of membrane area.

In chromaffin cells, capacitance measurements with an 868-Hz sine wave in the presence of the Na^+ channel blocker tetrodotoxin showed a transient capacitance increase following brief depolarizing pulses (Horrigan and Bookman, 1994). The amplitude of this phenomenon was correlated with the amplitude of peak I_{Na}. When both the capacitance change and I_{Na} were measured giving a pulse to +20 mV a slope of 8.3 fF/nA was obtained (Horrigan and Bookman, 1994). It should be noted that this phenomenon reflects a change in capacitance after a pulse relative to baseline. Thus, both measurements were performed at the same potential. The transient capacitance increase under these conditions was attributed to a change in gating charge movements due to inactivation with the decay to baseline reflecting recovery from inactivation (Horrigan and Bookman, 1994). Under these experimental conditions recovery from inactivation was slow (0.6 s), presumably due to the presence of tetrodotoxin. We have not systematically investigated capacitance changes after repolarization. Instead, our measurements were performed at quasi-steady-state at various potentials. Under these conditions the movement of gating charges directly contributes to membrane capacitance (Fernandez et al., 1982).

The voltage-dependent capacitance changes in nerve terminals showed at least two kinetically distinct components. A rapid capacitance change that occurred following step changes in membrane potential (ΔC_{step}) was followed by a gradual and slow capacitance decrease (ΔC_{slow}). ΔC_{step} was clearly correlated with the amplitude of Na^+ current present in the nerve terminal (Fig. 3, *B* and *C*). However, a voltage-dependent capacitance was also observed in a terminal that had no measurable Na^+ current (Fig. 5 *A*).

Voltage-dependent capacitance in the absence of Na^+ currents

The changes observed in the absence of detectable Na^+ currents were quite distinct from those observed in terminals with a strong Na^+ current. The capacitance showed a decrease by ~60 fF with increasing depolarization between

−60 and 0 mV (Fig. 4 *B*, *open circles*). Besides Na^+ channels, pituitary nerve terminals have various other voltage-dependent channels including at least three types of K^+ channels (Bielefeldt et al., 1992; Thorn et al., 1991; Wang et al., 1992a) and four types of Ca^{2+} channels (Lemos and Nowycky, 1989; Wang et al., 1997, 1999, 1992b). In our experimental conditions all these channels were maximally blocked or inactivated or both. However, following step changes in membrane potential the gating charges of the channels will still contribute the voltage-dependent capacitance. Presumably, all of these contribute to the voltage-dependent capacitance in a complex manner.

Voltage-dependent capacitance due to Na^+ channel gating currents

When a significant Na^+ current was present, ΔC_{step} was clearly correlated with the amplitude of the Na^+ current (Fig. 3, *B* and *C*). The correlation was almost perfect in the range of membrane potentials from −70 to −20 mV. This was consistent with a bell-shaped curve of ΔC_{step} versus V_m that showed a maximum near ~−40 mV (Figs. 4 *A* and 5 *B*). A correlation could appear accidentally if, for instance, both phenomena are proportional to the total membrane area of the nerve terminal. Interestingly, the correlation with total nerve terminal capacitance is extremely poor (Fig. 3 *D*), as is the correlation of Na^+ current amplitude with nerve terminal capacitance (data not shown). It is possible that the density of Na^+ channels in the nerve terminal membrane is extremely variable. Another possibility would be that the nerve terminals used in individual recordings have a variable amount of axonal membrane attached to them and that it is only the axonal membrane that contains Na^+ channels. The experiments described here cannot distinguish between these possibilities. Further evidence that ΔC_{step} is due to Na^+ channel gating currents is provided by the dibucaine experiments. Dibucaine blocks Na^+ currents as well as Na^+ channel gating currents (Gilly and Armstrong, 1980; Horrigan and Bookman, 1994). In the presence of dibucaine the capacitance change obtained with a voltage step from −82 to −52 mV was undistinguishable from that observed in a nerve terminal that had no detectable Na^+ current.

In terminals with a significant Na^+ current ΔC_{step} has all the properties expected for the movement of Na^+ channel gating charges. The capacitance changes were well fitted with Eq. 4 that assumed gating charge movement as expected from a simple two-state barrier model (Taylor and Bezanilla, 1979). A strong positive correlation exists between the maximum gating charge Q_G and the Na^+ current amplitude (Fig. 6 *A*). The capacitance change is blocked by dibucaine. A bell-shaped relationship exists between capacitance and membrane potential (Fig. 5 *B*) as found in frog skeletal muscle (Adrian and Almers, 1976) and squid giant axon (Armstrong and Bezanilla, 1973). In these studies, voltage-dependent capacitance was derived from the Na^+ channel gating currents at different pulse potentials. In squid axon voltage-dependent capacitance due to Na^+ channel gating charges was also measured using frequency domain admittance analysis (Fernandez et al., 1982). This method closely resembles the experimental conditions employed here because capacitance measurements were made at steady state, 155 ms after a voltage step, and should be compared with our protocol where ΔC_{step} was measured 100 ms after the voltage step. As in the nerve terminals studied here, the capacitance of the squid axon membrane shows a bell-shaped curve as a function of membrane potential and was attributed to the Na^+ channel gating charges. For similar holding potentials, the voltage-dependent capacitance in nerve terminals with strong Na^+ current has a shape remarkably similar to that measured in squid axon (Fernandez et al., 1982) with a peak near −40 mV and a decrease to about half the peak value near −70 mV.

The frequency domain measurements in squid axon allowed for a thorough investigation of the kinetic properties and showed that the frequency dependence of the voltage-dependent capacitance could be fit with a sum of two Debye relaxations corresponding to charge movements occurring with two time constants (Fernandez et al., 1982). It should be noticed, however, that one time constant was sufficient at hyperpolarized potentials and that the measurements were made at 7.5°C. The deviation from single-exponential behavior has recently been accounted for by applying Kramers' diffusion theory (Kramers, 1940) to the gating kinetics (Sigg et al., 1999). Although non-exponential kinetics are generally fitted better with a sum of two or more rather than a single exponential, a single exponential with a single lumped time constant may give a better and more robust description of the average kinetics (Austin et al., 1975; Lindau and Rüppel, 1983).

Comparison of ΔC_{step} with properties of Na^+ currents in pituitary nerve terminals

Na^+ currents in pituitary nerve terminals have been measured in whole terminals as well as outside-out patches (Jackson and Zhang, 1995). The peak Na^+ conductance is half-maximal near −20 mV in whole terminals and near −30 mV in excised patches. Fitting of Hodgkin-Huxley model parameters revealed a time constant τ_m of ~500 μs around −60 mV. We studied the frequency dependence of the capacitance difference associated with a membrane potential change from −82 to −122 mV because in this range contributions from phenomena other than Na^+ channel gating charges are minimal. The voltage-dependent capacitance due to Na^+ channel gating currents at −122 mV is ~6 times smaller than that at −82 mV when the average values for V_G and S_G are used in Eq. 2. The difference thus mainly reflects the capacitance due to gating charge movement at −82 mV. From the Hodgkin-Huxley parameters for Na^+

currents in rat pituitary nerve terminals (Jackson and Zhang, 1995) we estimate a value of ~90 μs for τ_m at −82 mV. This value is close to the time constant of 190 ± 90 μs that we obtained by fitting a Debye dispersion to the frequency dependence of ΔC_{step} (Fig. 6).

Slow capacitance decay in nerve terminals

The fast change in capacitance that occurs within 100 ms after a membrane potential step is followed by a slow capacitance decay ΔC_{slow} (Fig. 1). Following activation, Na^+ channels inactivate rapidly, and the inactivation process is associated with charge (Armstrong and Bezanilla, 1977; Bezanilla et al., 1991). In squid axon under conditions of prolonged depolarization two inactivation processes occur, termed fast and slow inactivation, both of which are associated with changes in gating charge mobility (Bezanilla et al., 1982). Fast inactivation develops within a few milliseconds whereas slow inactivation requires several seconds. At the time ΔC_{step} was measured in our experimental protocol, fast inactivation was presumably complete. A subsequent charge immobilization on a slow time scale associated with slow inactivation should manifest itself as a gradual capacitance decrease as observed here. ΔC_{slow} could thus correspond to the slow inactivation of the gating charge. Indeed, the ΔC_{slow} also displayed a bell-shaped voltage dependence with the maximum effect at ~−30 mV (Fig. 7 *A*). However, in contrast to ΔC_{step} the correlation between ΔC_{slow} and I_{Na} (Fig. 7 *B*) was weak, in particular between −50 and −30 mV. Because a comparable ΔC_{slow} was also detected in a nerve terminal that had no measurable Na^+ current, other phenomena must contribute to ΔC_{slow}. Presumably, these are slow inactivation processes occurring in voltage-gated K^+ and Ca^{2+} channels, which are present in the nerve terminal membrane in addition to voltage-gated Na^+ channels.

CONCLUSION

Using a lock-in amplifier we found that the capacitance in pituitary nerve terminals is voltage dependent. A significant part of the voltage-dependent capacitance is proportional to the Na^+ current present in the nerve terminal. The voltage and frequency dependence of this contribution suggests that it originates from the voltage-dependent movement of Na^+ channel gating charges.

This work has been supported by grants from the Deutsche Forschungsgemeinschaft (Li443/9–2) and the National Institutes of Health (1RO1-NS38200) to M.L. and by a Human Frontiers Science Program fellowship to G.K.

REFERENCES

Adrian, R. H., and W. Almers. 1976. The voltage dependence of membrane capacity. *J. Physiol. (Lond.).* 254:317–338.

Almers, W., and E. W. McCleskey. 1984. Nonselective conductance in calcium channels of frog muscle: calcium selectivity in a single pore. *J. Physiol. (Lond.).* 353:585–608.

Armstrong, C. M., and F. Bezanilla. 1973. Currents related to movement of the gating particles of the sodium channels. *Nature.* 242:459–461.

Armstrong, C. M., and F. Bezanilla. 1974. Charge movement associated with the opening and closing of the activation gates of the Na channels. *J. Gen. Physiol.* 63:533–552.

Armstrong, C. M., and F. Bezanilla. 1977. Inactivation of the sodium channel. II. Gating current experiments. *J. Gen. Physiol.* 70:567–590.

Austin, R. H., K. W. Beeson, L. Eisenstein, H. Frauenfelder, and I. C. Gunsalus. 1975. Dynamics of ligand binding to myoglobin. *Biochemistry.* 14:5355–5373.

Bezanilla, F., E. Perozo, D. M. Papazian, and E. Stefani. 1991. Molecular basis of gating charge immobilization in Shaker potassium channels. *Science.* 254:679–683.

Bezanilla, F., R. E. Taylor, and J. M. Fernandez. 1982. Distribution and kinetics of membrane dielectric polarization. I. Long-term inactivation of gating currents. *J. Gen. Physiol.* 79:21–40.

Bielefeldt, K., J. L. Rotter, and M. B. Jackson. 1992. Three potassium channels in rat posterior pituitary nerve terminals. *J. Physiol. (Lond.).* 458:41–67.

Cazalis, M., G. Dayanithi, and J. J. Nordmann. 1987. Hormone release from isolated nerve endings of the rat neurohypophysis. *J. Physiol. (Lond.).* 390:55–70.

Cole, K. S. 1972. Membranes, Ions, and Impulses. University of California Press, Berkeley.

Debus, K., J. Hartmann, G. Kilic, and M. Lindau. 1995. Influence of conductance changes on patch clamp capacitance measurements using a lock-in amplifier and limitations of the phase tracking technique. *Biophys. J.* 69:2808–2822.

Fernandez, J. M., F. Bezanilla, and R. E. Taylor. 1982. Distribution and kinetics of membrane dielectric polarization. II. Frequency domain studies of gating currents. *J. Gen. Physiol.* 79:41–67.

Fernandez, J. M., R. E. Taylor, and F. Bezanilla. 1983. Induced capacitance in the squid giant axon. Lipophilic ion displacement currents. *J. Gen. Physiol.* 82:331–346.

Fidler Lim, N., M. C. Nowycky, and J. Bookman. 1990. Direct measurement of exocytosis and calcium currents in single vertebrate nerve terminals. *Nature.* 344:449–451.

Gillis, K. D. 1995. Techniques for membrane capacitance measurements. *In* Single-Channel Recording, 2nd ed. B. Sakmann and E. Neher, editors. Plenum Press, New York. 155–198.

Gilly, W. F., and C. M. Armstrong. 1980. Gating current and potassium channels in the giant axon of the squid. *Biophys. J.* 29:485–492.

Giovannucci, D. R., and E. L. Stuenkel. 1997. Regulation of secretory granule recruitment and exocytosis at rat neurohypophysial nerve endings. *J. Physiol. (Lond.).* 498:735–751.

Herrington, J., and R. J. Bookman. 1994. Pulse Control V4.3: Igor XOPs from Patch Clamp Data Acquisition. University of Miami Press, Miami.

Horrigan, F. T., and R. J. Bookman. 1994. Releasable pools and the kinetics of exocytosis in adrenal chromaffin cells. *Neuron.* 13: 1119–1129.

Hsu, S.-F., and M. B. Jackson. 1996. Rapid exocytosis and endocytosis in nerve terminals of the rat posterior pituitary. *Biophys. J.* 494:539–553.

Jackson, M. B., and S. J. Zhang. 1995. Action potential propagation and propagation block by GABA in rat posterior pituitary nerve terminals. *J. Physiol. (Lond.).* 483:597–611.

Kilic, G., A. Stolpe, and M. Lindau. 1996. A slowly activating voltage-dependent K^+ current in rat pituitary nerve terminals. *J. Physiol. (Lond.).* 497:711–725.

Kramers, H. A. 1940. Brownian motion in a field of force and the diffusion model of chemical reactions. *Physica.* 7:284–304.

Lemos, J. R., and M. C. Nowycky. 1989. Two types of calcium channels coexist in peptide-releasing vertebrate nerve terminals. *Neuron.* 2:1419–1426.

Lindau, M. 1991. Time-resolved capacitance measurements: monitoring exocytosis in single cells. *Quart. Rev. Biophys.* 24:75–101.

Lindau, M., and E. Neher. 1988. Patch-clamp techniques for time-resolved capacitance measurements in single cells. *Pflügers Arch. Eur. J. Physiol.* 411:137–146.

Lindau, M., and H. Rüppel. 1983. Evidence for conformational substates of rhodopsin from kinetics of light-induced charge displacement. *Photobiochem. Photobiophys.* 5:219–228.

Lindau, M., E. L. Stuenkel, and J. J. Nordmann. 1992. Depolarization, intracellular calcium, and exocytosis in single vertebrate nerve endings. *Biophys. J.* 61:19–30.

Neher, E., and A. Marty. 1982. Discrete changes of cell membrane capacitance observed under conditions of enhanced secretion in bovine adrenal chromaffin cells. *Proc. Natl. Acad. Sci. U.S.A.* 79:6712–6716.

Sigg, D., H. Qian, and F. Bezanilla. 1999. Kramers' diffusion theory applied to gating kinetics of voltage-dependent channels. *Biophys. J.* 76:782–803.

Taylor, R. E., and F. Bezanilla. 1979. Comments on the measurement of gating currents in the frequency domain. *Biophys. J.* 26:338–340.

Thorn, P. J., X. Wang, and J. R. Lemos. 1991. A fast, transient K^+ current in neurohypophysial nerve terminals of the rat. *J. Physiol. (Lond.).* 432:313–326.

Wang, G., G. Dayanithi, S. Kim, D. Hom, L. Nadasdi, R. Kristipati, J. Ramachandran, E. L. Stuenkel, J. J. Nordmann, R. Newcomb, and J. R. Lemos. 1997. Role of Q-type Ca^{2+} channels in vasopressin secretion from neurohypophysial terminals of the rat. *J. Physiol. (Lond.).* 502: 351–363.

Wang, G., G. Dayanithi, R. Newcomb, and J. R. Lemos. 1999. An R-type Ca(2+) current in neurohypophysial terminals preferentially regulates oxytocin secretion. *J. Neurosci.* 19:9235–9241.

Wang, G., P. Thorn, and J. R. Lemos. 1992a. A novel large-conductance Ca^{2+}-activated potassium channel and current in nerve terminals of the rat neurohypophysis. *J. Physiol. (Lond.).* 457:47–74.

Wang, X., S. N. Treistman, and J. R. Lemos. 1992b. Two types of high-threshold calcium currents inhibited by ω-conotoxin in nerve terminals of the rat neurohypophysis. *J. Physiol. (Lond.).* 445:181–199.